

### Strain Effects in Acyl Transfer Reactions. Part 4.<sup>1</sup> Kinetic Analysis of the Reaction of Imidazole Buffer Solutions with $\beta$ -Propiolactone using a Novel Graphical Method for Branched, Series Reactions

By G. Michael Blackburn \* and David Duce, Department of Chemistry, The University, Sheffield S3 7HF

The imidazole-catalysed hydrolysis of  $\beta$ -propiolactone (oxetan-2-one) proceeds by formation and subsequent hydrolysis of 1-(3-hydroxypropionyl)imidazole. There is concurrent production of 1-(2-carboxyethyl)imidazole as the major product. Continuous monitoring of the acylimidazole intermediate enables a complete kinetic analysis to be carried out for all three processes by application of a novel graphical method for the solution of the integrated rate equation for branched, series reactions.

The formation of the acylimidazole intermediate involves nucleophilic attack of imidazole at C-1 and is catalysed by imidazole. Its hydrolysis proceeds *via* water, specific acid, specific base, and imidazole acid and base catalytic processes for which the rate constants are almost identical in value with those for the corresponding terms for hydrolysis of 1-acetylimidazole. *N*-Alkylation of imidazole by  $\beta$ -propiolactone is subject to specific but not general base catalysis.

STRAIN effects at the acyl centre of small-ring lactones<sup>1</sup> and amides<sup>2,3</sup> provide a valuable opportunity for examination of the influence of conformational and angular distortions on well-characterised catalytic processes. The reasonable expectation that such influences might be reflected in the behaviour of natural products has been borne out by the similarity between the rate laws for the catalytic aminolysis of *N*-aryl- $\beta$ -lactams<sup>3</sup> and of benzylpenicillin.<sup>4</sup> The possibility that enzymes employ strain as an important feature of their catalytic behaviour<sup>5</sup> presents a more daunting challenge to mechanistic analysis and to modelling in catalytic systems.

There is, however, no doubt about the special role of histidine residues in peptidolytic and esterolytic enzymic activities.<sup>6</sup> Equally, the sharp contrast between the nucleophilic catalysis of aryl carboxylate ester hydrolyses by imidazole and its general base catalysis in the case of

aliphatic carboxylates is well defined<sup>7</sup> and holds good also for models of enzyme systems.<sup>8</sup> Accordingly we directed our attention to the hydrolysis and aminolysis of small-ring lactones and, in particular, to the role of imidazole as catalyst in such processes.

The influence of imidazole on the hydrolysis of  $\beta$ -propiolactone has been investigated both in water and in ice by Butler and Bruice.<sup>9</sup> They found it to be an uncomplicated case of nucleophilic catalysis readily monitored by the standard hydroxamate assay.<sup>10</sup> When we re-examined this reaction system, the results obtained from pH-stat monitoring of the course of hydrolysis indicated the existence of a more complicated kinetic system. That inference was confirmed by the direct observation of the formation of an intermediate and its subsequent decay which exhibited the u.v.

<sup>5</sup> Cf. W. P. Jencks, 'Catalysis in Chemistry and Enzymology,' McGraw-Hill, New York, 1969, p. 282.

<sup>6</sup> D. M. Blow, *Accounts Chem. Res.*, 1976, **9**, 145.

<sup>7</sup> J. F. Kirsch and W. P. Jencks, *J. Amer. Chem. Soc.*, 1964, **86**, 837.

<sup>8</sup> G. M. Blackburn and H. L. H. Dodds, *J. Chem. Soc. (B)*, 1971, 826.

<sup>9</sup> A. R. Butler and T. C. Bruice, *J. Amer. Chem. Soc.*, 1964, **86**, 313.

<sup>10</sup> F. Lipmann and L. C. Tuttle, *J. Biol. Chem.*, 1945, **159**, 21.

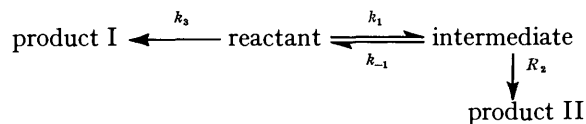
<sup>1</sup> Part 3, G. M. Blackburn and H. L. H. Dodds, *J.C.S. Perkin II*, 1974, 377.

<sup>2</sup> G. M. Blackburn and J. D. Plackett, *J.C.S. Perkin II*, 1972, 1366.

<sup>3</sup> G. M. Blackburn and J. D. Plackett, *J.C.S. Perkin II*, 1973, 981.

<sup>4</sup> A. F. Martin, J. J. Morris, and M. I. Page, *J.C.S. Chem. Comm.*, 1976, 495.

absorption curve characteristic of an acylimidazole,  $\lambda_{\max}$  245 nm.<sup>1</sup> Approximate kinetic analysis of this phenomenon showed that it stemmed from a branched, series reaction system.



Neither the graphical solution for series reactions<sup>11</sup> nor its development by Fersht and Jencks<sup>12</sup> could be applied in this case because of the similarity in the rates of formation and decay of the intermediate monitored and because of the simultaneous operation of the branched part of the reaction scheme. We therefore developed a novel graphical method for the solution of this problem which appears to be generally applicable in those cases for which  $k_{-1}$  is negligible. We here describe the application of that method and the mechanistic interpretation of the kinetic description it provides for the reaction of  $\beta$ -propiolactone in aqueous imidazole buffers.

#### EXPERIMENTAL

**Materials.**— $\beta$ -Propiolactone was purified by distillation immediately before use, its purity being routinely checked by g.l.c. Imidazole was recrystallised from benzene and stored *in vacuo* prior to use. Glass-distilled water was used throughout and standard solutions were prepared using AnalaR grade potassium chloride and Convol hydrochloric acid solution (Hopkin and Williams).

**Apparatus.**—N.m.r. proton spectra were recorded at 100 MHz using a Varian HA 100 and i.r. spectra with a Perkin-Elmer 157G instrument for Nujol mulls. U.v. spectra were recorded using a Cary 14 spectrophotometer and kinetic runs were continuously monitored using either a Unicam SP 1800 or a Gilford 240 spectrophotometer, both having cell temperatures controlled by water circulated from a Haake Fe thermostat.

**Kinetic Measurements.**—All reactions were carried out in 10 mm quartz cuvettes at  $298 \pm 0.05$  K and unit ionic strength (KCl). They were initiated by the addition of neat  $\beta$ -propiolactone (0.3–0.9  $\mu$ l) with efficient stirring to the appropriate buffer solution (3.0 ml) containing  $2 \times 10^{-5}$ M ethylenediaminetetra-acetic acid to give a maximal optical density reading in the range 0.5–1.5 at 245 nm. The pH of reaction solutions was measured before and after each kinetic run using a Radiometer PHM26 instrument in conjunction with a G2222B glass electrode.

All reactions were monitored continuously at 245 nm until there was no further significant change in optical density. They all showed an increase in absorption followed by its return to almost, but not exactly, the initial optical density (OD) of the imidazole buffer solution. Preliminary kinetic analysis was carried out on the terminal portion of the absorption curve in the usual way<sup>11</sup> and also on the initial slope.

For complete analysis, plots of  $\log(\text{OD})$  against  $\log(\text{time})$  were fitted to standard curves generated as described below to provide the shape factor,  $\beta$ , and the two axes shift

\* The value of the extinction coefficient used for B is  $3 \times 10^3$ , as determined for acetylimidazole (E. R. Stadtman in 'The Mechanism of Enzyme Action,' eds. W. D. McElroy and B. Glass, Johns Hopkins Press, Baltimore, 1954, p. 581).

factors. These were manipulated to give the three rate constants,  $k_1$ ,  $k_2$ , and  $k_3$  as described below.

**Product Analysis.**—The conversion of  $\beta$ -propiolactone into hydracrylic acid in simple hydrolysis<sup>1</sup> and in imidazole buffers<sup>9</sup> has been described previously. Completed reaction solutions showed the presence of a second, major product which was identified by t.l.c. and by spectroscopic comparison with an authentic sample of 1-(2-carboxyethyl)-imidazole.

**1-(2-Carboxyethyl)imidazole.**— $\beta$ -Propiolactone (oxetan-2-one) (3.1 g) was added slowly to a stirred solution of imidazole (3.4 g) in anhydrous ethanol at room temperature. The white crystalline precipitate was filtered off, washed, and dried (1.7 g). Recrystallisation from water gave 3-[3-(2-carboxyethyl)imidazolio]propionate, m.p. 473–474 K, identical with the material prepared as below. Evaporation of the ethanolic filtrate gave an oil (5.8 g), which afforded crystals on trituration with ether. Repeated crystallisation from spectroscopic grade ethanol gave 1-(2-carboxyethyl)imidazole (1.1 g), m.p. 419–420 K (lit.,<sup>13</sup> 422–423 K) (Found: C, 51.1; H, 5.75; N, 19.7. Calc. for  $C_6H_8N_2O_2$ : C, 51.4; H, 5.75; N, 20.0%),  $\tau$  1.82 (s, H-2), 3.07 (d,  $J$  8.5 Hz, H-4 and -5), 6.10 (t,  $J$  6 Hz, N-CH<sub>2</sub>), and 7.76 (t,  $J$  6 Hz, CH<sub>2</sub>·CO<sub>2</sub><sup>-</sup>),  $\nu_{\max}$  3140w (N<sup>+</sup>H) and 1720br,s cm<sup>-1</sup> (CO<sub>2</sub><sup>-</sup>),  $\lambda_{\max}$  (H<sub>2</sub>O) 210 nm ( $\epsilon$   $4.1 \times 10^3$ ).

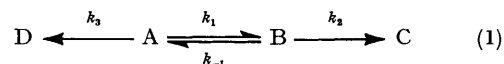
**3-[3-(2-Carboxyethyl)imidazolio]propionate.**— $\beta$ -Propiolactone (1 g) was added to a stirred solution of imidazole (1 g) in anhydrous ether (200 ml). After 2 days the solution was evaporated *in vacuo*. The solid was crystallised repeatedly from dry ethanol to yield the product, m.p. 471 K (1.1 g) (Found: C, 50.75; H, 5.4; N, 13.2.  $C_9H_{12}N_2O_4$  requires C, 50.95; H, 5.4; N, 13.2%),  $\tau$  1.14br (s, H-2), 2.75 (m, H-4 and -5), 5.47 (dt,  $J_{1,2}$  6.5,  $J_{1,4}$  2.6 Hz, N-CH<sub>2</sub>), and 7.13 (t,  $J$  6.5 Hz, CH<sub>2</sub>·CO<sub>2</sub><sup>-</sup>),  $\nu_{\max}$  1715br,m cm<sup>-1</sup> (CO<sub>2</sub><sup>-</sup>),  $\lambda_{\max}$  (H<sub>2</sub>O) 212 nm ( $\epsilon$   $3.9 \times 10^3$ ).

#### RESULTS

**Kinetic Treatment.**—The imidazole-catalysed hydrolyses were carried out at concentrations of buffer from 0.1 to 1.0M and pH values from 6.3 to 8.6 (Table). Over the whole

| % Im <sub>free</sub> | No. of runs | [Im] <sub>tot</sub> /mol l <sup>-1</sup> | pH   |
|----------------------|-------------|--|------|
| 10                   | 5           | 0.2–1.0                                  | 6.27 |
| 18                   | 5           | 0.2–1.0                                  | 6.53 |
| 28                   | 6           | 0.1–0.9                                  | 6.83 |
| 50                   | 5           | 0.1–0.8                                  | 7.20 |
| 70                   | 4           | 0.2–0.9                                  | 7.62 |
| 86                   | 7           | 0.1–1.0                                  | 8.04 |
| 96                   | 6           | 0.1–1.0                                  | 8.58 |

range, the optical density at 245 nm showed a steady increase followed by an exponential decay (Figure 1). Preliminary estimates of the rate constants for the formation of acylimidazole (initial slope) and its decay (final slope)<sup>12</sup> coupled with the estimation of the maximum concentration of acylimidazole formed\* established the operation of a branched, series reaction scheme [equation (1)] in which A, C, and D, are materials transparent at 245 nm and B is the species monitored.



<sup>11</sup> A. A. Frost and R. G. Pearson, 'Kinetics and Mechanism,' Wiley, New York, 1961, p. 166.

<sup>12</sup> A. R. Fersht and W. P. Jencks, *J. Amer. Chem. Soc.*, 1970, **92**, 5432.

<sup>13</sup> J. B. Jones and J. M. Young, *Canad. J. Chem.*, 1970, **48**, 1566.

The rate equation for the variation in concentration of B with time can be integrated by means of Laplacian transforms to give the general solution (2), in which  $a = k_1 +$

$$[B] = k_1[A_0]\{e^{-\frac{1}{2}t(a-b)} - e^{-\frac{1}{2}t(a+b)}\}/b \quad (2)$$

$k_2 + k_3 + k_{-1}$  and  $b = [a^2 - 4(k_1k_2 + k_2k_3 + k_3k_{-1})]^{1/2}$ . In this work, the simplification  $k_{-1} \rightarrow 0$  was adopted (see

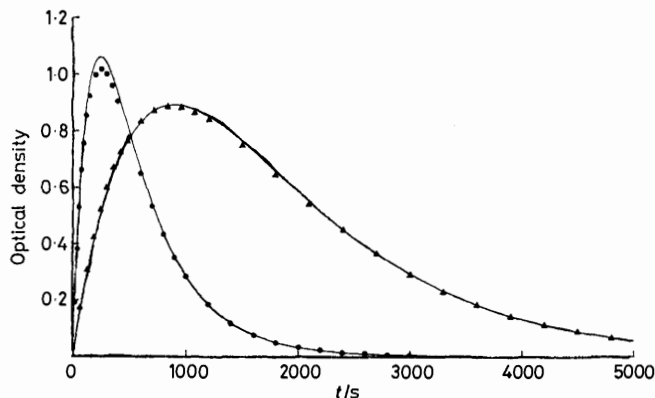


FIGURE 1 Plots of absorbance at 245 nm against time for acylimidazole formation and disappearance at pH 8.04 in imidazole buffers at 0.2M (▲) and 0.09M (●) total concentration; solid lines calculated from data of equations (8)–(10) and equation (3)

Discussion section).\* Consequently, equation (2) reduces to (3), for which the logarithmic form (4) is appropriate for the case  $k_2 > (k_1 + k_3)$  and the form (5) is appropriate when  $k_2 < (k_1 + k_3)$ .

$$[B] = k_1[A_0]\{e^{-(k_1+k_3)t} - e^{-k_2t}\}/(k_2 - k_1 - k_3) \quad (3)$$

$$\log[B] = \log\{k_1[A_0]/(k_2 - k_1 - k_3)\} + \log[e^{-(k_1+k_3)t} - e^{-k_2t}] \quad (4)$$

$$\log[B] = \log\{k_1[A_0]/(k_1 + k_3 - k_2)\} + \log[e^{-k_2t} - e^{-(k_1+k_3)t}] \quad (5)$$

Substitution of the parameters  $\beta = k_2/(k_1 + k_3)$ ,  $\tau = (k_1 + k_3)t$ , and  $\gamma = k_1[A_0]/|(k_1 + k_3 - k_2)|$  transforms equation (4) into (6) and equation (5) into (7) for values of

$$\log[B] = \gamma + \log(e^{-\tau} - e^{-\beta\tau}) \quad (6)$$

$$\log[B] = \gamma + \log(e^{-\beta\tau} - e^{-\tau}) \quad (7)$$

$\beta$  greater than unity and less than unity respectively.

Setting  $\gamma = 0$  provides a form of the equation which can be plotted graphically to give a family of curves for values of  $\beta \neq 1$  (Figure 2), generated in this work by means of a Hewlett-Packard 9125B calculator plotter.

When the absorption data at 245 nm are plotted logarithmically as a function of  $\log(\text{time})$ , experimental curves are produced each of which can be fitted optimally by inspection to a particular member of the family of calculated curves. This superposition makes it possible to evaluate three parameters for each experimental curve: the shape factor,  $\beta$ , the horizontal shift factor,  $\alpha$ , and the vertical shift factor,  $\gamma$ , relating the origins. From these parameters the three rate constants can be extracted directly:

$$k_1 = 10^{(\alpha+\gamma)}(1-\beta)/[A_0]; \quad k_2 = \beta 10^\alpha;$$

$$k_3 = 10^\alpha(1-10^\gamma)/(1-\beta)/[A_0].$$

It should be noted that  $(k_1 + k_3)$  and  $k_2$  can be evaluated

without making use of the extinction coefficient for the intermediate B, but partitioning to give  $k_1$  and  $k_3$  separately demands this information.

Such a graphical analysis thus provides a novel, simple solution for evaluation of the rate constants in the branched

series reaction scheme,  $D \xleftarrow{k_2} A \xrightarrow{k_1} B \xrightarrow{k_3} C$ , the utility of which is established in the sequel.

*Kinetic Analysis.*—In practice, all the experimental curves could be fitted to calculated curves with shape factors in the range  $0.3 < \beta < 0.9$  for absorption data usually spanning two decades in magnitude. The horizontal shift factor,  $\alpha$ , was susceptible to accurate evaluation,  $\beta$  could be assigned to within  $\pm 0.05$ , so that the error in  $[A_0]$  provided the greatest source of error—a result of the techniques adopted in handling the volatile, labile, and carcinogenic  $\beta$ -propiolactone.

Values of the observed pseudo-unimolecular rate constants,  $k_1$ ,  $k_2$ , and  $k_3$ , were thus obtained for each of the

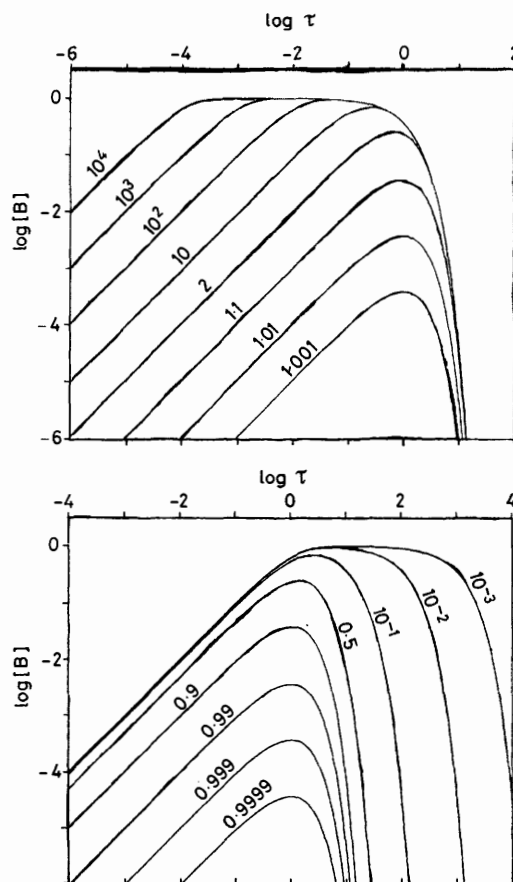


FIGURE 2 Representative plots of  $\log [B] = \log(e^{-\beta\tau} - e^{-\tau})$  for values of  $\beta$  greater (upper diagram) and less than unity (lower diagram)

separate kinetic runs (Table) and were thereafter analysed by standard methods.

Plots of the value of  $k_1$  as a function of total imidazole buffer concentration show a greater than first-order dependence of the formation of the acylimidazole intermediate B

\* If  $k_3 \rightarrow 0$  then equation (2) reduces to the form adopted by Fersht and Jencks<sup>12</sup> for the analysis of the reversible, series kinetic scheme appropriate to the pyridine-catalysed hydrolysis of acetic anhydride.

on buffer concentration (Figure 3). Plots of the apparent second-order rate constants for this process showed linear

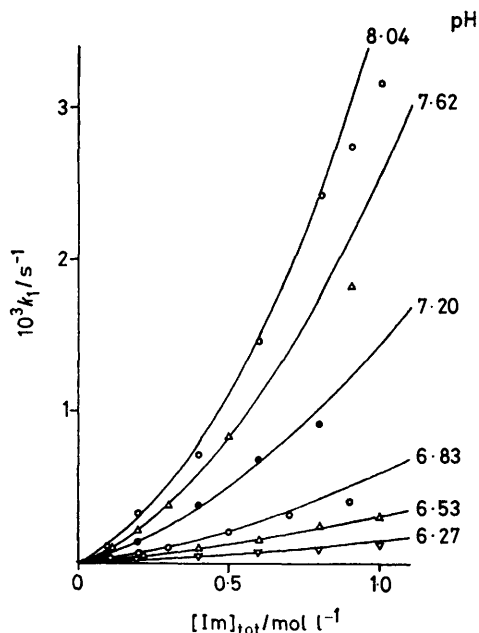


FIGURE 3 Variation of the apparent first-order rate constants for the formation of 1-(3-hydroxypropionyl)imidazole (B) as a function of imidazole concentration at pH values indicated; slopes calculated from equation (8)

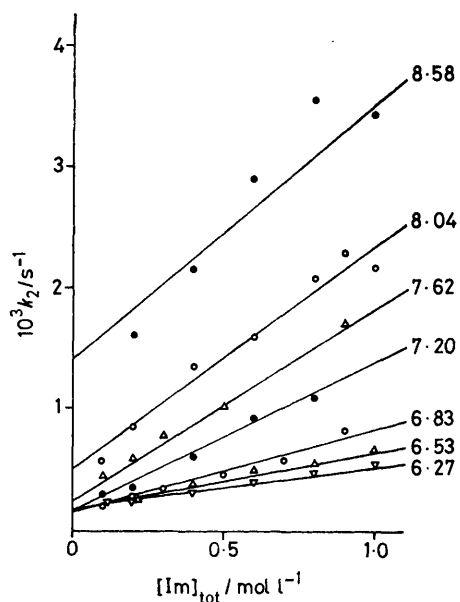


FIGURE 4 Variation in the apparent first-order rate constants for the disappearance of the acylimidazole (B) as a function of imidazole concentration at pH values indicated; slopes calculated from equation (9)

dependence on the concentration of imidazole free base with intercepts which were essentially constant over the pH range investigated. Linear regression analysis of these data provided the second- and third-order rate constants

<sup>14</sup> W. P. Jencks and J. Carriolo, *J. Biol. Chem.*, 1959, **234**, 1272.

for the nucleophilic reaction of imidazole at C-1 of  $\beta$ -propiolactone according to equation (8) (Im = imidazole).

$$k_{1(\text{obs})} = (1.00 \pm 0.04) \times 10^{-3} [\text{Im}_{\text{free}}] + (3.83 \pm 0.11) \times 10^{-3} [\text{Im}_{\text{free}}]^2 \text{ s}^{-1} \quad (8)$$

The values of the observed rate constant for the disappearance of B,  $k_2$ , were plotted as a function of the concentration of imidazole buffer to give straight lines for which both slope and intercept varied as a function of pH (Figure 4). Plotting the intercepts against pH (Figure 5) provided a very good correlation for the buffer-independent hydrolysis of B with the theoretical curve calculated for the hydrolysis of acylimidazole under similar conditions.<sup>14</sup> The slopes of the curves were plotted as a function of the mole fraction of imidazole free base in the buffers used (Figure 6) whence linear regression analysis provided the catalytic rate constants for the influence of the imidazolium ion (general acid

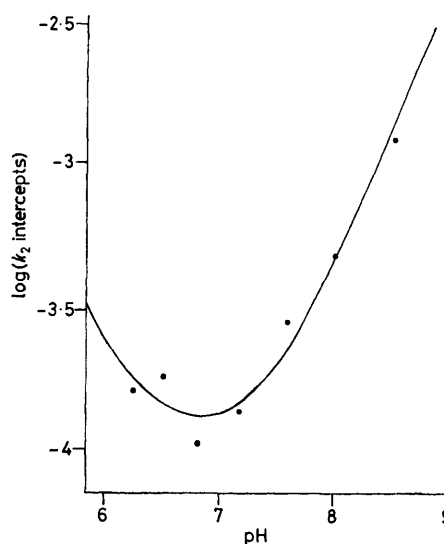


FIGURE 5 Logarithmic plot of the rate of hydrolysis of acylimidazole (B), extrapolated to zero buffer concentration, against pH; theoretical curve calculated for  $k_{\text{obs}} = 8.3 \times 10^{-5} + 190 [\text{H}^+] + 320 [\text{OH}^-] \text{ s}^{-1}$

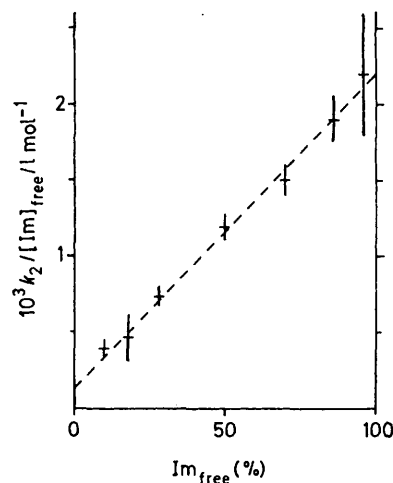


FIGURE 6 Variation in the apparent second-order rate constants for the disappearance of acylimidazole (B) as a function of imidazole buffer composition; broken line obtained by linear regression analysis

catalysis) and imidazole free base (general base catalysis) on the hydrolysis of B. These rate constants sum to provide equation (9) for the rate of hydrolysis of the acylimidazole intermediate B from which the theoretical curves in Figures 4 and 5 were derived.

$$k_{2(\text{obs})} = 8.3 \times 10^{-5} + 190[\text{H}^+] + 320[\text{OH}^-] + (1.4 \pm 0.3) \times 10^{-4}[\text{ImH}^+] + (2.09 \pm 0.06) \times 10^{-3}[\text{Im}] \text{ s}^{-1} \quad (9)$$

Finally, plots of the apparent first-order rate constants for the consumption of  $\beta$ -propiolactone not involving an acylimidazole intermediate,  $k_3$ , as a function of buffer concentration

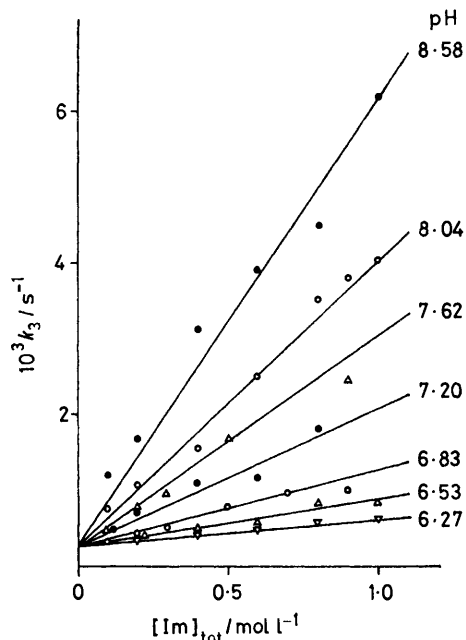


FIGURE 7 Variation in the apparent first-order rate constants for the formation of D from  $\beta$ -propiolactone as a function of imidazole concentration; theoretical slopes calculated from equation (10)

gave straight lines whose intercepts were effectively independent of pH. Below pH 8, the slopes were proportional to the mole fraction of imidazole in the free base form but above pH 8 they showed a direct dependence on the hydroxide ion concentration. The common intercept (Figure

7) was obtained as the weighted mean of the intercepts for the seven independently calculated curves, whose slopes were then redetermined by linear regression analysis for this constant intercept and as a function of hydroxide ion concentration. This provided the second- and third-order terms of the rate equation (10) corresponding to attack of imidazole on  $\beta$ -propiolactone other than at C-1.

$$k_{3(\text{obs})} = (2.4 \pm 1) \times 10^{-4} + (3.7 \pm 0.2) \times 10^{-3}[\text{Im}] + (590 \pm 120)[\text{Im}][\text{OH}^+] \text{ s}^{-1} \quad (10)$$

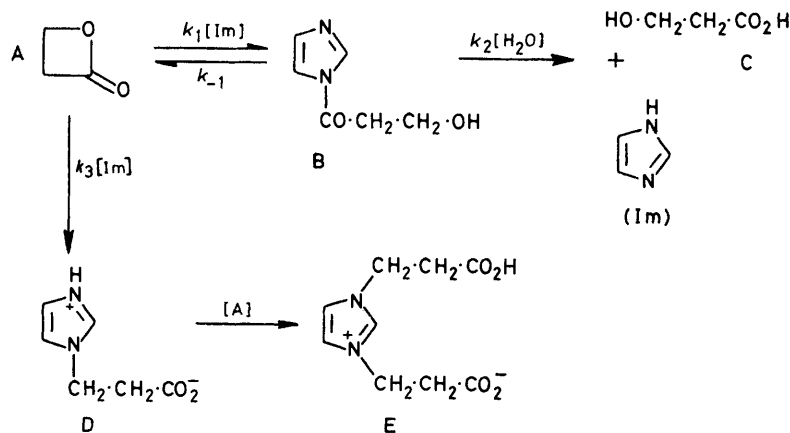
All the above results were associated with an apparent  $pK_a$  value of 7.15 for imidazole and, where appropriate, assumed a  $pK_a$  value of 3.6 for acylimidazole.<sup>14</sup> From the combined values of  $k_1$ ,  $k_2$ , and  $k_3$  thus obtained, theoretical curves were calculated by means of equation (3) for the observed variation in optical density as a function of time for two specimen reactions (Figure 1).

#### DISCUSSION

In the course of our experiments on the hydrolysis of  $\beta$ -propiolactone, we investigated the effect of tertiary amines.<sup>1</sup> In the case of imidazole solutions at pH 9–10, pH-stat monitoring of the reaction revealed significant deviations from first-order behaviour which indicated the formation of a neutral intermediate and its subsequent hydrolysis to anionic products. This behaviour is consistent with the fast transformation of  $\beta$ -propiolactone, A, into 3-hydroxypropionylimidazole, B, by nucleophilic attack at C-1 with subsequent slower hydrolysis of B to give hydracrylic acid C as the ultimate product. This hypothesis was readily verified by scanning the light absorption of reaction mixtures containing A in imidazole buffer solutions in the pH range 6.3–8.6 to reveal the characteristic u.v. spectrum of an acylimidazole intermediate, presumably B, as a transient.

In terms of equation (1), the hydroxylamine assay procedure used by Butler and Bruce<sup>9</sup> would provide kinetic data on the function  $d([\text{A}] + [\text{B}])/dt$  and not on  $d[\text{B}]/dt$  as they anticipated.

*Kinetic Treatment.*—The complete analysis of the four rate constants in equation (1) should follow in principle from deconvolution of the data for  $d[\text{B}]/dt$  given that  $[\text{B}_0]$ ,  $[\text{C}_0]$ , and  $[\text{D}_0]$  are zero. In practice, however, the



number of successful solutions of such a scheme is limited in cases where the formation and decay of the intermediate observed, B, have similar velocities.<sup>12</sup> Moreover, the system under present investigation has the additional complexity that A not only reacts by alkylation of imidazole to give D but by further alkylation of D to form the betaine E, which is the principal product in ethereal solution.

Two reasonable simplifications were applied to the reaction scheme to ease its kinetic analysis. First, the formation of E was neglected since it can be assumed to be only a minor product under the first-order conditions of reaction of A with a large excess of imidazole and also since both D and E are effectively transparent at the wavelength, 245 nm, used to monitor the formation of B. Secondly, the reversion of B to  $\beta$ -propiolactone can be discounted in view of the strain energy needed to regenerate the oxetanone ring. Thus the complex rate equation (2) simplifies to (3), in which the three independent variables can be separately evaluated by application of the novel graphical solution for a branched, series reaction scheme described above.

In practice, the double logarithmic plots of the experimental data could be fitted equally well to calculated curves (Figure 2) for values of  $\beta$  either in the range 0.2–0.9 or in the complementary range for  $\beta > 1$ . If values less than unity are assigned to  $\beta$ , then the initial rise in light absorption corresponds to the formation of B and the subsequent fall in absorption represents its hydrolysis. Alternatively, if  $\beta$  is greater than unity, then the rise in absorption relates to the hydrolysis of B and the subsequent fall in absorption is associated with the rate of formation of B.

In their elegant study of the pyridine-catalysed hydrolysis of acetic anhydride, Fersht and Jencks were obliged to resolve this unavoidable ambiguity by appealing to chemical intuition concerning the expected dependences of the two rate processes on the concentrations of the various reactants since the extinction coefficient,  $\epsilon$ , for the *N*-acetylpyridinium ion could be neither determined nor estimated.<sup>12</sup> In this study, the extinction coefficient for B can be assumed to have a value close to that for 1-acetylimidazole.\* However, that assumption is not capable of resolving the ambiguity in this case because the maximum concentration of B is determined not only by the magnitude of the rate constants for processes directly involved in its formation and disappearance,  $k_1$  and  $k_2$ , but also by the magnitude of the rate constant for the branched feature,  $k_3$ . Thus, for instance, if  $k_3$  is dominant, no B is formed.

We were therefore obliged to calculate one set of rate constants for both alternative sets of values of  $\beta$ . In the event, only those derived from values of  $\beta$  less than unity provided a coherent picture and their alternatives were discarded. The justification for that choice is manifest in the sequel, above all in the quality of fit between experimental data profiles and those calculated by combination of all the rate constants here determined in the integrated rate equation (3).

*Formation of 3-Hydroxypropionylimidazole.*—The observed rate constants for the formation of B show a greater than first-order dependence on the concentration of imidazole (Figure 3). Analysis of these data by standard procedures provides a second-order rate constant for acylation of imidazole by  $\beta$ -propiolactone of  $1.0 \times 10^{-3} \text{ l mol}^{-1} \text{ s}^{-1}$  which is in close agreement with that of  $1.2 \times 10^{-3} \text{ l mol}^{-1} \text{ s}^{-1}$  previously determined for the corresponding acylation of 1-methylimidazole under comparable conditions.<sup>1</sup> In addition, the imidazole reaction shows autocatalysis with a third-order rate constant of  $3.83 \times 10^{-3} \text{ l}^2 \text{ mol}^{-2} \text{ s}^{-1}$  [equation (8)]. The magnitudes of these two rate constants show that  $\beta$ -propiolactone has a similar reactivity to both *p*-tolyl and *p*-methoxyphenyl acetates with respect to acylation of imidazole.<sup>7</sup>

Kirsch and Jencks have used structure–reactivity correlations to draw a clear distinction between the role of imidazole as a nucleophile towards acyl esters with good leaving groups and as a general base towards those with poor leaving groups.<sup>7</sup> We have previously made reference to the value of this distinction in relation to the catalysis by imidazole of the hydrolysis of *N*-acetyl-*O*-formylserinamide.<sup>8</sup> That study of a model system for the action of serine esterases and proteases supported the designation of the function of a histidine residue in the active site of such enzymes as a general-base catalyst. However, the present results amply demonstrate that imidazole can change role dramatically and act as a nucleophile towards an acyl ester in which a weak leaving group of normal  $pK_a$  value is activated by strain effects which are relieved on hydrolysis of the ester.

This study thus shows that the role of histidine in transacylation reactions of enzymes cannot safely be resolved by appealing to structure–activity relationships.

It is not possible to decide from the evidence available here whether the second imidazole species acts as a general base in rate-determining nucleophilic attack of imidazole at C-1 of A or as a general catalyst to promote a ring-opening process in transformation of a presumed tetrahedral intermediate into B. This ambiguity may, however, relate to two aspects of the kinetic data which are not adequately explained by the scheme proposed.

First, at the highest concentration of imidazole used, there is often a decrease in the observed rate of reaction as compared with that predicted (Figure 3). Such a feature is characteristic of a change in mechanism for the aminolysis of esters with respect to the formation and breakdown of a tetrahedral intermediate.<sup>15</sup> Secondly, the  $k_1$  data for the reaction of A at the highest pH value investigated (8.6) are smaller than those predicted by equation (8) by up to 50%. This must be in part a result of the combination of errors in their calculation since at this pH they are a minor part of the composite rate constant ( $k_1 + k_3$ ). However this  $k_1$  divergence is uniformly negative and is outside the limits of accuracy

\* See footnote \* p. 1494.

<sup>15</sup> G. M. Blackburn and W. P. Jencks, *J. Amer. Chem. Soc.*, 1968, **90**, 2638.

of evaluation of the data at every other point in the total analysis. It is thus possible that at high pH there is a change in rate-determining step for either the formation of B from A or the reversion of (B) to (A), *i.e.*  $k_{-1}$  cannot be neglected.

*Hydrolysis of 3-Hydroxypropionylimidazole.*—The apparent rate constants for the hydrolysis of B show a simple dependence on the concentration of imidazole buffers (Figure 4). The imidazole-independent hydrolysis of B, determined by extrapolation to zero buffer concentration at several different pH values, agrees well with that of acetylimidazole itself, as shown by the close correlation between the experimental data for B and the calculated curve for the hydrolysis of acetylimidazole at 298 K calculated from the classical work of Jencks and Carriuolo<sup>14</sup> (Figure 5).

Examination of the buffer-catalysed component of this reaction in the usual way (Figure 6) shows that it originates predominantly from general-base catalysis but that there is also a significant contribution from general-acid catalysis. The rate constant for general-base catalysis,  $2.09 \times 10^{-3} \text{ l}^2 \text{ mol}^{-2} \text{ s}^{-1}$ , lies between the values determined for acetylimidazole at ionic strength 0.2M (KCl) ( $2.3 \times 10^{-3} \text{ l}^2 \text{ mol}^{-2} \text{ s}^{-1}$ )<sup>14</sup> and at ionic strength 1.0M ( $\text{Me}_4\text{N}^+\text{Cl}^-$ ) ( $1.5 \times 10^{-3} \text{ l}^2 \text{ mol}^{-2} \text{ s}^{-1}$ ),<sup>16</sup> both at 298 K. Although general-acid catalysis of the hydrolysis of acetylimidazole was not reported in the original study,<sup>14</sup> it has since been recognised both for substituted imidazoles<sup>17</sup> and for acetylimidazole itself<sup>16</sup> and is usually *ca.* 20% of the rate constant for imidazole general-base catalysis of hydrolysis.

This indirect analysis\* of the hydrolysis of 1-(3-hydroxypropionyl)imidazole correlates quantitatively in every respect with the pattern of behaviour expected for a simple acylimidazole and thus provides both a kinetic confirmation of the structure of intermediate B and a justification for the selection of values of  $\beta$  less than unity for the solution of equation (7).

*Reaction of  $\beta$ -Propiolactone at C-3.*—In contrast to our study of the reaction of  $\beta$ -propiolactone and *N*-methylimidazole,<sup>1</sup> it was not feasible in this work to quantify the formation of 1-(2-carboxyethyl)imidazole, D, from A in reaction mixtures. The problem relates to the zwitterionic nature of the product, to the presence of traces of the bis-adduct, E, and to the difficulty in separation of B and E from the larger quantities of imidazole, imidazole hydrochloride, and salt necessarily present in completed reaction mixtures. Consequently, the processes grouped under the rate constant  $k_3$  in the Scheme must include nucleophilic attack of imidazole at C-3 of  $\beta$ -propiolactone and general catalysis of the hydro-

lysis of B by BA12 and BA2 processes in indeterminate relative proportions

Analysis of these rate constants in the usual way shows (Figure 7) a linear dependence of  $k_{3\text{obs}}$  on imidazole concentration. The imidazole-independent reaction of A is essentially pH-independent and gives a rate constant of  $2.4 \times 10^{-4} \text{ s}^{-1}$ , which is in fair agreement with that reported<sup>1</sup> for the pH-independent hydrolysis of  $\beta$ -propiolactone. The buffer-dependent process is directly proportional to the concentration of imidazole at lower pH but under the most alkaline conditions used there is a rate enhancement which is apparently dependent on the concentration of hydroxide.

It can be deduced that the predominant buffer reaction at moderate pH values involves nucleophilic attack of imidazole at C-3 of A to form D. The maximum rate constant for this process ( $3.7 \times 10^{-3} \text{ l mol}^{-1} \text{ s}^{-1}$ ) is remarkably close to that previously determined for the corresponding reaction of A with 1-methylimidazole ( $3.6 \times 10^{-3} \text{ l mol}^{-1} \text{ s}^{-1}$ ).<sup>1</sup>

The third-order rate constant [equation (10)] most probably relates to the reaction of the imidazole anion ( $\text{p}K_a$  14.7) at C-3 of A, corresponding to a bimolecular rate constant of  $3 \times 10^3 \text{ l mol}^{-1} \text{ s}^{-1}$ , since there is no evidence for imidazole catalysis of the alkylation of imidazole. Taken overall,  $k_3/k_1$  implies that up to 90% of the products of reaction of imidazole with  $\beta$ -propiolactone result from attack at C-3 and this is consistent with the results of examination of completed reaction solutions.

*Conclusion.*—The reaction of imidazole buffers with  $\beta$ -propiolactone involves two sequential processes and a third simultaneous one. The kinetic behaviour of all three has been examined across a range of pH and imidazole concentrations and mechanisms have been assigned to each of the several rate constants determined. Seven of these rate constants show very good quantitative agreement with those observed for comparable processes and evaluated by direct methods.

These facts and the excellent correspondence between the observed kinetic data and the light absorption profile calculated from these rate constants and the integrated rate equation (3) (Figure 1) fully validate the usefulness of the novel, graphical method of analysis developed here for the solution of this problem as generally applicable to the analysis of branched, series reaction systems.

We thank Dr. Julian Kinderlerer for generous assistance in attempts to achieve a computer-based analysis of this system.

[7/235 Received, 10th February, 1977]

\* It is noteworthy that this analysis of  $k_2$  is independent of any assumption concerning the extinction coefficient,  $\epsilon$ , for intermediate B.

<sup>16</sup> D. G. Oakenfull and W. P. Jencks, *J. Amer. Chem. Soc.*, 1971, **93**, 178.

<sup>17</sup> T. H. Fife, *J. Amer. Chem. Soc.*, 1965, **87**, 4597.